Available online at www.sciencedirect.com
ScienceDirect
Ceramics International 33 (2007) 1495–1502
CERAMICS INTERNATIONAL
www.elsevier.com/locate/ceramint

Properties of BST ceramics prepared by high temperature hydrothermal process

K.A. Razak, A. Asadov *, W. Gao

Department of Chemical and Materials Engineering, The University of Auckland, Private Bag 92019, Auckland, New Zealand

Received 12 December 2005; received in revised form 22 April 2006; accepted 2 June 2006
Available online 18 September 2006

Abstract

Barium strontium titanate (BST) was produced in a pressure vessel at 220 °C using the hydrothermal technique. Ba and Sr concentrations, temperature, reaction time and Ti concentration were varied to study the effects of processing on the formation of BST. The chemical composition and crystal structure were analysed by X-ray diffractometry. Peak fitting software was used to separate contributions from different BST phases and to calculate the relative volumes of the phases. From the obtained data Ba losses relative to initial Ba:Sr ratio were estimated. It was found that the amount of Ti was critical for BST phase formation. A small amount of Ti, less than 0.19 mol/l, in a Ba rich solution leads to a single-phase structure, as Sr greatly outperforms Ba. An increase of Ti above 0.225 mol/l decreases Ba losses and creates a solid solution of two phases: one is tetragonal, almost Sr-free, and the other is cubic BST. When the initial concentration of Sr is increased above 30% the obtained BST became triple-phased with different Ba:Sr ratios.

Keywords: A. Powders: chemical preparation; B. X-ray methods; Grain size; D. $BaTiO_3$ and titanates

1. Introduction

There are three commonly used processing techniques to produce BST powders: conventional solid state [1,2], sol–gel [3] and hydrothermal methods [4,5]. The solid-state technique requires a calcination step at high temperature to produce a crystalline solid solution, and it can be contaminated due to repeated grinding. The obtained powder particles are usually big in size and wide in range [6,7]. The sol–gel technique is capable of producing nano-sized powders, but most of the starting chemicals are expensive, sensitive to moisture, and require a particular processing environment to control the properties. The powder produced is normally amorphous [3,8]. Unlike both techniques, the hydrothermal technique is able to produce nano-crystalline powders at low temperature (as low as 80 °C); the powder particle size range is small, and the method is relatively inexpensive [4,5,9]. However, it is hard to control the stoichiometry of the final products produced by this technique.

Roeder and Slamovich [4], using a low temperature hydrothermal reaction, found that BST powders produced from a solution with an almost stoichiometric ratio of Ba:Sr and TiO_2, was a biphasic compound of Ba-rich and Sr-rich phases. Decreasing the initial content of Ti led to a Sr-rich single phased BST. Deshpande et al. [5] suggested the use of excess TiO_2 to obtain the right stoichiometry of BST. Both results are not comparable for they used different starting materials. Chloride based materials require preparation of $BaSr(OH)_2$ solution by reaction with a mineralizer [4]. During filtration, to obtain a clear solution, some of the Ba^{2+} and Sr^{2+} were lost. On the other hand, in nitride-based chemicals, there was no filtration step, thus the stoichiometry in the solution remained the same until the hydrothermal reaction [5].

In this study we carried out a high temperature hydrothermal reaction in a pressure vessel at 220 °C [9] using chloride based Ba and Sr. TiO_2 source was 100% anatase as it reacts faster than rutile [6]. It was expected that the high temperature and high pressure incorporated in this method could decrease losses in the reagents and improve the quality of the final product. The aim of this paper was to investigate the influence of different parameters on the stoichiometry of the BST powders. The main emphasis was on Ba to Sr and Ba + Sr to Ti ratios and the

* Corresponding author. Tel.: +64 9 3737599x87258; fax: +64 9 3737463.
E-mail address: a.asadov@auckland.ac.nz (A. Asadov).

0272-8842/$32.00
doi:10.1016/j.ceramint.2006.06.011

duration of the reaction, as they were known to significantly affect the electrical properties of the obtained BST [10,11]. The Ba to Sr ratio was limited in the range of 1.0–0.7 as these samples had the Curie point close to room temperature. The obtained data were compared with the results of a low temperature hydrothermal reaction [4].

2. Sample preparation

The high temperature hydrothermal technique used in the experiments is schematically shown in Fig. 1 [10,11]. Starting materials $BaCl_2{\cdot}2H_2O$ and $SrCl_2{\cdot}6H_2O$ were added to distilled water containing 1.2 M of NaOH and continuously stirred at 80 °C for 2 h. The NaOH concentration was calculated from the following chemical equations:

$$BaCl_2{\cdot}2H_2O + 2NaOH \rightarrow Ba(OH)_2 + 2NaCl + 2H_2O \quad (1)$$

$$SrCl_2{\cdot}6H_2O + 2NaOH \rightarrow Sr(OH)_2 + 2NaCl + 6H_20 \quad (2)$$

Distilled water, before the reaction, was previously boiled for 30 min to remove dissolved CO_2. The hydration water incorporated in $BaCl_2$ and $SrCl_2$ was taken into account during the preparation to achieve a concentration (molarity, M) of Ba + Sr = 0.6 M. Different mol ratios of Ba:Sr from 1.0:0.0 to 0.7:0.3 were used in the experiments. The solution was then filtered and mixed with different amount of TiO_2 powder (100% anatase). The concentration of anatase varied from 0.125 to 0.250 M. This gives relative concentrations of (Ba + Sr)/TiO_2 from 4.8 (calculated as 0.6 M/0.125 M) to 2.4 (as 0.6 M/0.25 M). The final solution was poured into the Teflon lined pressure vessel and then placed in a pre-heated oven at 220 °C for 8–48 h. The obtained powder was filtered, washed three times using water of pH 2 adjusted by NH_4OH, filtered again and, finally, dried.

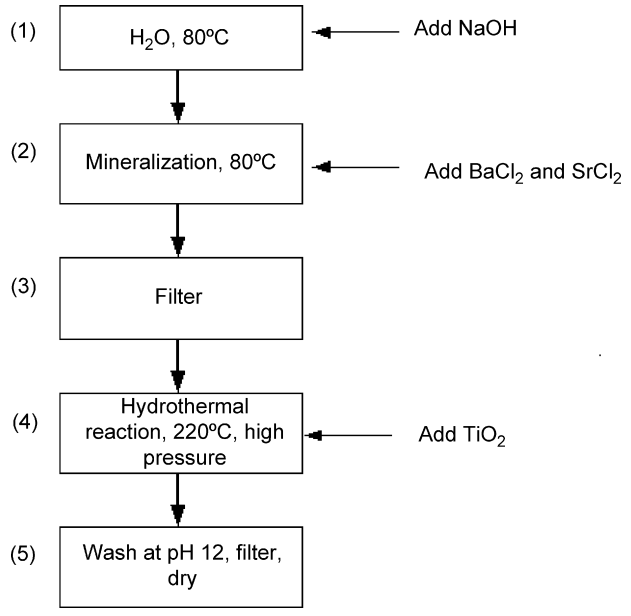

Fig. 1. Flowchart of BST preparation by the high temperature hydrothermal method.

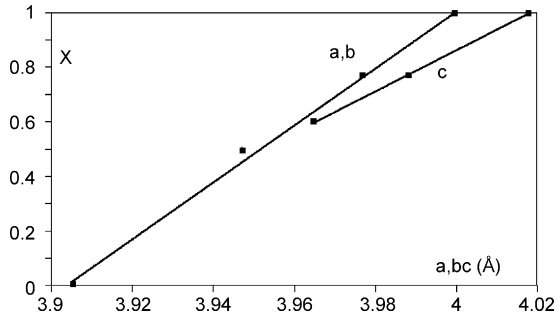

Fig. 2. $x(d)$ dependence, where d is a, b or c lattice parameters, obtained using data from 79-2265, 34-0411, 44-0093, 39-1395 and 79-0175 PDF numbers.

Finally, the prepared powders were heat treated for 2 h at 550 °C to free the incorporated water [12].

3. Experimental technique

Crystal structure of the obtained samples was studied using a D8 Advance Bruker X-ray diffractometer with Cu Kα radiation. In the case of a two-phase structure the obtained spectra were analysed with Fityk 0.0.4 software (http://www.fityk.sf.net) in order to separate contributions of $Ba_xSr_{1-x}TiO_3$ compounds with different x values. The parameter x was then determined from the Vegard's law using data from 79-2265, 34-0411, 44-0093, 39-1395 and 79-0175 PDF files. From Fig. 2 it can be seen that the calibration graph $x(a, b)$, where a and b are cell parameters, has a linear relation in the whole range of x from 0 to 1. It is also seen that the tetragonal structure undergoes a phase transition into a cubic phase in the region of $x = 0.6$.

Microstructure of the powders was studied by Philips XL-30S FEG-SEM and Philips CM12 TEM. Thermogravimetric measurements were performed using Shimadzu TGA-50.

4. Experimental results

4.1. 550 °C heat treatment

It is known that hydrothermally prepared powders have a considerable amount of water incorporated in the perovskite structure [12]. This may lead to a substantial error in measuring the lattice parameters by XRD. Usually the hydroxyl defects disappear after a heat treatment. Thermogravimetric analysis confirmed that the 500 °C peak, which was associated with water [12], disappeared after a heat treatment at 550 °C for 2 h. Fig. 3 shows the changes of (1 1 0) peak after the heat treatment. It is seen that the peak becomes narrower and its maximum shifted to higher angles.

4.2. Filter content

The residue collected from the filter (step 2 in Fig. 1) was analysed using XRD, and was found to have a composition of ~70% $BaCO_3$, ~20% NaCl, 7% Sr(OH)Cl, 3% SrO. These percentages were obtained from a sample with an initial Ba:Sr mol ratio 0.9:0.1 (Table 1), using semi-quantitative analysis of

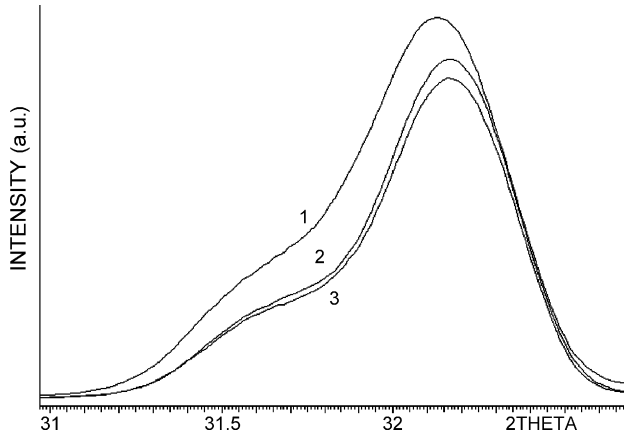

Fig. 3. (1 1 0) peak of Ba:Sr = 0.8:0.2 sample: (1) as prepared, (2) heat treated for 1 h at 550 °C, and (3) heat treated at 550 °C for 2 h.

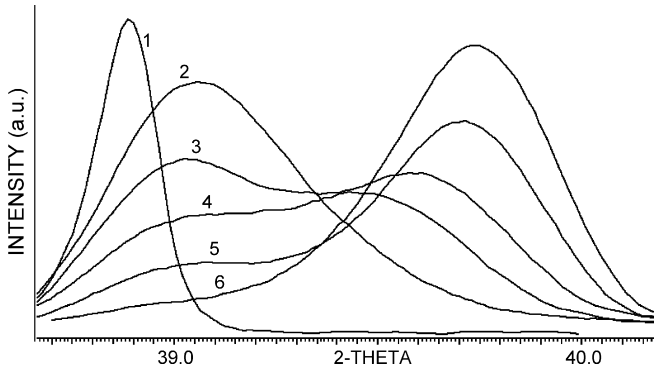

Fig. 4. (1 1 1) peak of Ba-pure (1) and five samples prepared with different Ba:Sr mol ratios of 0.9:0.1 (2), 0.85:0.15 (3), 0.8:0.2 (4), 0.75:0.25 (5), and 0.7:0.3 (6). The experimental curves were smoothed for a better view.

the EVA DiffracPlus Basic software. It is seen that the ratio between Ba and Sr in the solid precipitates is 0.88:0.12, which is roughly the same as in the original mixture. It means that these losses do not upset very much the initial chemical balance between Ba and Sr in the solution.

4.3. Ba:Sr ratio

XRD analysis of the samples with Ba:Sr mol ratios of 0.9:0.1, 0.85:0.15, 0.8:0.2 and 0.75:0.25 (while the Ba + Sr to TiO_2 ratio for all was fixed at 2.4, and duration of the hydrothermal reaction was 16 h), showed that the compounds consisted of $Ba_xSr_{1-x}TiO_3$ with two different values of x. Fig. 4 shows the (1 1 1) peak of the six samples. It can be seen that the peak splits into two when %Sr increases. The position of the first peak does not change much being close to the (1 1 1) peak of $BaTiO_3$, while the second peak increases in intensity and shifts to higher angles with increasing amount of Sr. This type of behaviour could not be explained by the structural changes, as the (1 1 1) peak may shift, but should not split, during the $BaTiO_3$ (tetragonal) to $Ba_xSr_{1-x}TiO_3$ (cubic) symmetry transformation. It is, therefore, reasonable to assume that the sample structure is not uniform and there are two types of crystal structures, each with a different amount of Sr. Since the peaks of the two compounds are close to each other, fitting software was used to separate them (Fig. 5). We can derive the amount of Ba, x, in the structure using Vegard's law (Fig. 2) from the position of the calculated (2 0 0) peak. Similar calculations were then applied independently to (1 1 0, 1 0 1) peak to compare the results. These data were finally compared with the cell parameters computed from the whole spectrum fit. The obtained results are listed in Table 1a and b.

The grain size was calculated from the full width at half maximum (FWHM) of the peaks, using the Schrerrer's relation:

$$t = \frac{0.9\lambda}{(B_m^2 - B_s^2)^{1/2}\cos\theta} \quad (3)$$

Table 1
Data obtained from the XRD analysis of (1 1 0, 1 0 1) (a) and (2 0 0) (b) peaks of samples prepared with different initial mol ratios of Ba:Sr

Ba:Sr	2-th$_1$	2-th$_2$	S_1/S_2	t_1	t_2	x_1	x_2	Ba loss (%)
(a)								
0.1:0.0	31.50^0			45				
0.9:0.1	31.64^0	31.93	72/28	23	21	0.93	0.59	7
0.85:0.15	31.64^1	32.04	55/45	20	20	0.95	0.45	12
0.8:0.2	31.67^2	32.09	43/57	20	22	0.85	0.38	22
0.75:0.25	31.71^2	32.17	28/72	17	24	0.81	0.29	31

Ba:Sr	2-th$_1$	2-th$_2$	S_1/S_2	Ba$_1$:Sr$_1$	Ba$_2$:Sr$_2$	t_1	t_2	x_1	x_2	Ba loss (%)
(b)										
0.1:0.0	45.27					33				
0.9:0.1	45.39	45.80	67/33	62:5	19:14	16	13	0.93	0.57	9
0.85:0.15	45.37	45.97	50/50	47:3	22:28	15	16	0.94	0.43	16
0.8:0.2	45.48	46.10	45/55	38:7	18:37	12	16	0.85	0.33	24
0.75:0.25	45.52	46.21	30/70	24:6	16:54	11	20	0.81	0.23	35

2-th$_1$ and 2-th$_2$ are positions of the first and second peaks calculated from the peak fit (Fig. 4). Indexes ^{0}, ^{1} and ^{2} at 2-th$_1$ indicate the origin of the (1 1 0, 1 0 1) peak determined from a whole spectrum fit. Index ^{0} indicates a double (1 1 0, 1 0 1) peak, index ^{1}—(1 1 0) peak and index ^{2}—(1 0 1) peak. Ba$_1$:Sr$_1$ and Ba$_2$:Sr$_2$ are ratios of the elements in the two phases calculated according to the formulas (5) and (6). S_1/S_2 are relative areas under the peaks, t_1 and t_2 are the grain size calculated according to the formula (3) in nm, parameters x_1 and x_2 show the amount of Ba in $Ba_xSr_{1-x}TiO_3$ compounds and are obtained from the 2-th values and Vegard's law (Fig. 2). Ba loss shows how much of Ba in the final product is unaccounted for compare with the initial value in percent.

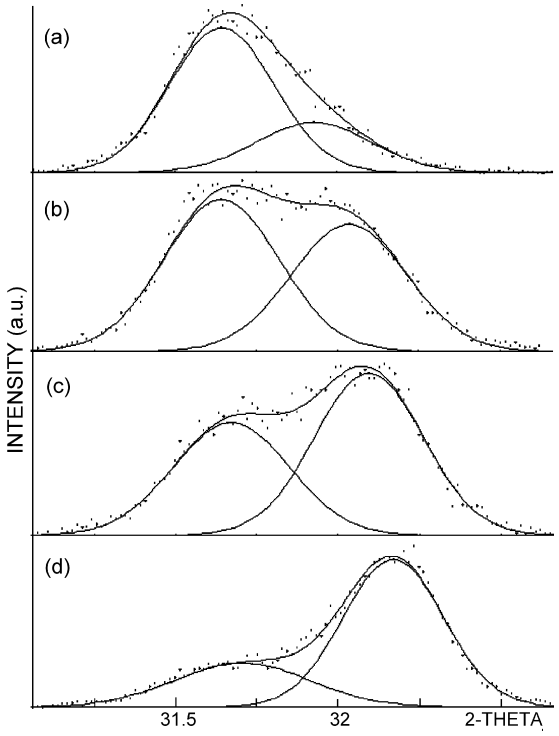

Fig. 5. Spectra of (1 1 0, 1 0 1) peak of samples prepared with Ba:Sr of (a) 0.9:0.1, (b) 0.85:0.15, (c) 0.8:0.2 and (d) 0.75:0.25. Solid lines are theoretical peaks obtained from the best fit.

where λ is the X-ray wavelength, B_m and B_s are the experimental and instrumental FWHMs values, respectively.

The calculated crystal size, t, is very small, in the range of 11–20 nm (Table 1b), and different for the two types of crystals in the four samples with varying Ba contents. In the initial case of 90% Ba, 67% of the powder consisted of Ba-rich $Ba_{0.93}Sr_{0.07}TiO_3$ crystals with 17 nm in size and 33% of Ba-poor $Ba_{0.57}Sr_{0.43}TiO_3$ with $t_2 = 13$ nm. In the final case of the 75% Ba sample, the situation is opposite: 30% of Ba-rich crystals have a very small size of 11 nm, and 70% $Ba_{0.23}Sr_{0.77}TiO_3$ crystals are 20 nm in size. A similar trend, with slightly different values, is obtained from the analysis of (1 1 0, 1 0 1) peak (Table 1a). Crystal sizes calculated from (2 0 0) peak are smaller, probably because they came from the longitudinal direction, compared to the lateral direction (1 1 0, 1 0 1); and the shape of the crystals, according to the SEM pictures (see Fig. 6a), is a plate-like. TEM study confirmed that the smallest particles in the powder are in the calculated range (Fig. 6b). The big particles, possibly, have a complex globular structure.

Table 1 shows that the XRD peaks of 90:10 and 85:15 Ba:Sr samples were successfully described by the peak fit software. For higher Sr content (20–25%) there is a small difference in the parameters calculated from the fit of (1 1 0, 1 0 1) and (2 0 0) peaks (compare Table 1a and b). The whole spectrum fit of these samples has a relatively high figure of merit coefficient (difference between the experimental and a calculated curve). The fitting error becomes too large for the 30% Sr sample. It could only be described assuming a three (or more) phase solid solution. Fitting the experimental peaks in this case becomes nontrivial, as there is more than one way to choose fitting

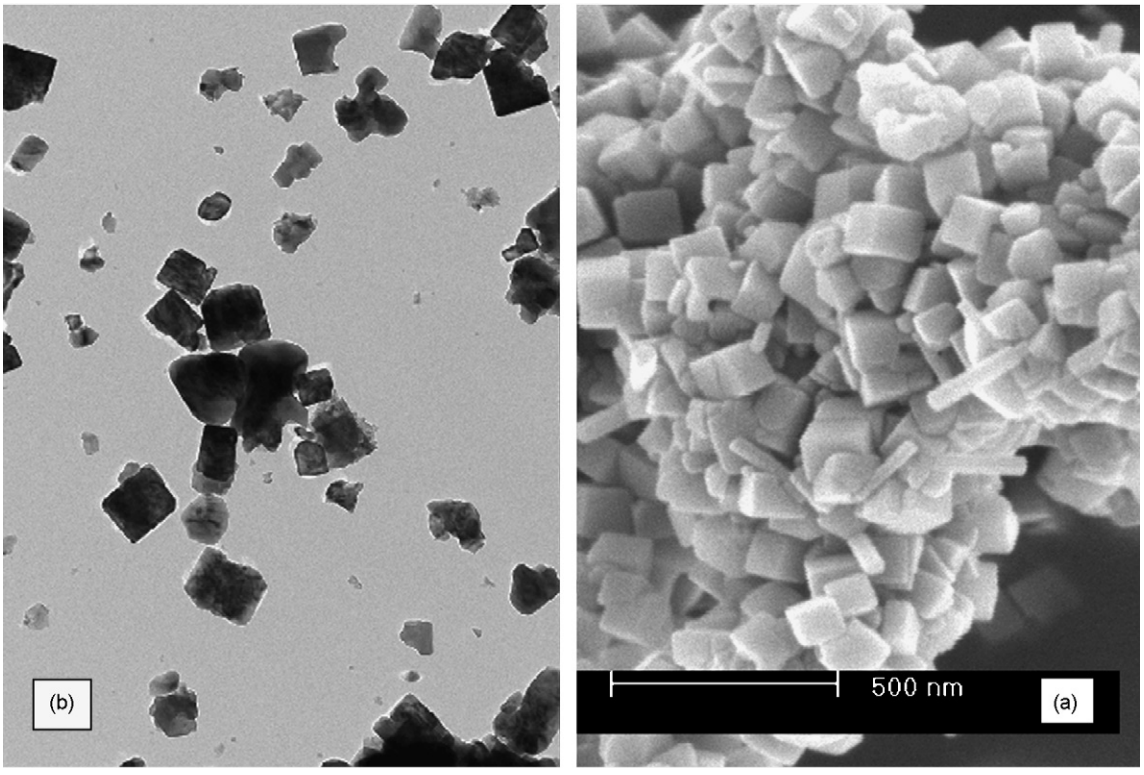

Fig. 6. Micrographs of typical BST powders: (a) SEM and (b) TEM.

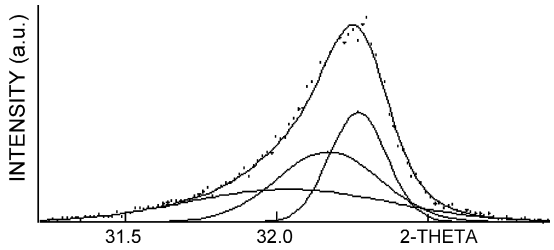

Fig. 7. (1 1 0) peak of Ba:Sr = 0.7:0.3 sample. Solid lines are theoretical peaks obtained from the best fit.

parameters. Fig. 7 shows one of the most likely ways to fit the experimental data.

Assuming that the X-ray absorption coefficients of the phases in the final products are similar, since their structures are similar, then the areas S under the peaks should be proportional to the relative amount of the phase. Taking this into account and deriving a parameter x for the phases from the positions of the peaks (Fig. 2), we can calculate the ratio between Ba and Sr after the reaction. For example, in the case of the sample with initial mol ratio Ba:Sr = 0.8:0.2, which has a 45/55 ratio of the areas of the two peaks and $x_1 = 0.85$ and $x_2 = 0.33$ (Table 1b), one can write for the final compound:

$$\begin{aligned} &45\%\ Ba_{0.85}Sr_{0.15}TiO_3 + 55\%\ Ba_{0.33}Sr_{0.67}TiO_3 \\ &\quad = (45\% \times 0.85 + 55\% \times 0.33)Ba \\ &\quad + (45\% \times 0.15 + 55\% \times 0.67)Sr \\ &\quad = 56\%Ba + 44\%Sr. \end{aligned} \tag{4}$$

This is 24% smaller than the initial value of 80% Ba. It can be seen from Table 1 and Fig. 8 that the Ba losses increase with

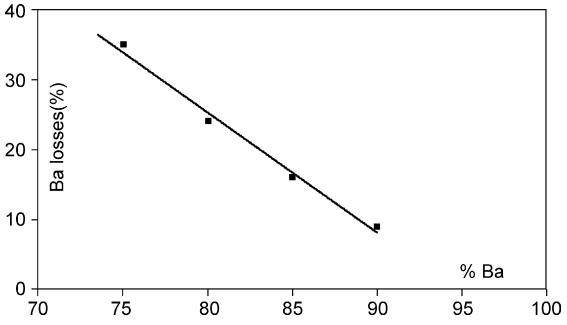

Fig. 8. Ba losses vs. Ba mol ratio in the initial solution in percent (Table 1b).

increasing of Sr content in the original mixture. This behaviour can be explained by a higher mobility of Sr ions compared to Ba ions [4]. The derived values 56%Ba + 44%Sr show the relative amounts of Ba and Sr in the mixture of the two phases. One can also calculated the distribution of Ba and Sr inside the phases (Ba_1:Sr_1 and Ba_2:Sr_2). One can write for the first Ba-rich phase:

$$\begin{aligned} &Ba_1 = 45\% \times 0.85 = 38\%, \quad \text{and} \\ &Sr_1 = 45\% \times 0.15 = 7\% \end{aligned} \tag{5}$$

and for the second, Sr-rich phase:

$$\begin{aligned} &Ba_2 = 55\% \times 0.33 = 18\%, \quad \text{and} \\ &Sr_2 = 55\% \times 0.67 = 37\%. \end{aligned} \tag{6}$$

The calculated results Ba_1:Sr_1 and Ba_2:Sr_2 (see Table 1b) show that the amount of Sr_1 (3–7%) in the first, Ba-rich phase, and amount of Ba_2 (18–22%) in the second, Sr-rich, phase, do not change with the initial Ba:Sr mol ratio. When the amount of Sr in the initial solution increased, all the contributed Sr went only to produce more Sr-rich phase; or, similarly, all initially substituted Ba was taken from the Ba-rich phase.

4.4. (Ba + Sr)/TiO_2 ratio

The (Ba + Sr)/TiO_2 ratio was changed during the experiments as it was known to affect the stoichiometry of BST powder [4]. There were four samples prepared with different ratios of (Ba + Sr)/TiO_2: 4.79, 3.20, 2.66 and 2.40. The initial mol ratio of Ba to Sr was 0.9:0.1 for all samples. The resulting data are listed in Table 2. It is seen that for the smallest value of Ti (4.79) the resulting compound is Ba-deficient and single phased. As the amount of Ti increased to 3.20, x increased from 0.64 to 0.77. A further increase in Ti (2.40) reduces the Ba loss to minimum (Fig. 9), but the final powder becomes two phased with the first phase almost Sr free, and the second one with $x = 0.6$ (Fig. 10). The threshold value of (Ba + Sr)/TiO_2 for a two-phase solid solution is about 3, indicating poor atomic diffusion even at the reaction temperatures of 220 °C (compare with 80 °C in [4]) and under an elevated pressure.

It is not clear why the two-phase structure appears and why its content is $x_1 = 1$ and $x_2 = 0.6$, though it is interesting to highlight that the tetragonal $BaTiO_3$ and cubic $Ba_{0.60}Sr_{0.40}TiO_3$ each accommodate the maximum possible amount of Ba in both structures (Fig. 2). Table 2 shows that more Ti, (Ba + Sr)/TiO_2 = 2.4, did not change the phase content x_1 and x_2, but the

Table 2
Data obtained from the XRD analysis of the (1 1 0, 1 0 1) peaks of samples prepared with different amount of TiO_2

(Ba + Sr)/TiO_2	2-th$_1$	2-th$_2$	S_1/S_2	t_1	t_2	x_1	x_2	Ba loss (%)
4.8	31.88			18		0.64		26
3.19	31.78			17		0.78		12
2.65	31.62	31.93	81/19	20	19	0.98	0.59	0
2.4	31.62	31.92	71/29	20	19	0.98	0.60	3

Concentration ratio (Ba + Sr)/TiO_2 is given in M/M, 2-th$_1$ and 2-th$_2$ are positions of the first and second peaks calculated from the peak fit, S_1/S_2 are relative areas under the peaks, t_1 and t_2 are sizes of the crystals calculated according to the formula (1) in nm, parameters x_1 and x_2 show amount of Ba in $Ba_xSr_{1-x}TiO_3$ compounds and are obtained from 2-th and Vegard's law (Fig. 2), Ba loss shows how much of Barium in the final product is unaccounted for compare with the initial value of 90% in percent.

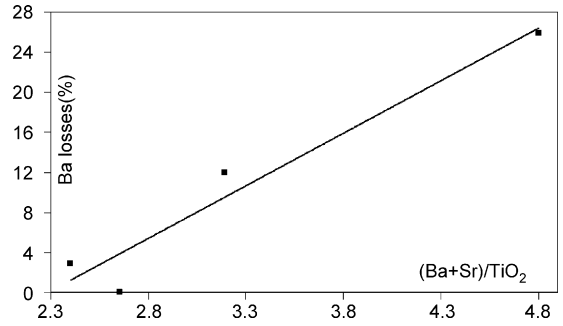

Fig. 9. Ba losses vs. (Ba + Sr)/TiO_2 ratio in the initial solution.

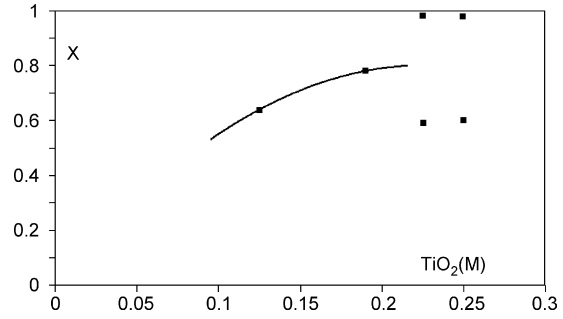

Fig. 10. Dependence of TiO_2 concentration in the initial solution in moles vs. phase parameter x of the final BST. The solid line is a calculated trendline assuming also that $x = 0$ when $TiO_2 = 0$.

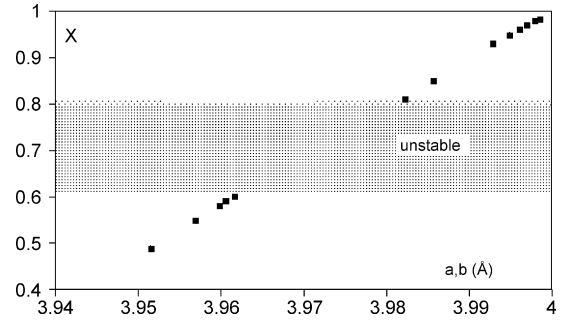

Fig. 11. Dependence of a and b cell parameters in angstroms of all the two-phased samples studied in the experiments vs. their structural parameter x. The dashed area shows the gap in the data appeared, presumably, because this structure is thermodynamically unfavourable in the hydrothermal reaction.

volume of the second phase increased, as the relative area under the peak S_2 increased to 29%. Considering also that a third phase, in the previous experiment, appeared when the first Ba-rich phase content, x_1, decreased to 0.80 (Fig. 7), one may assume that the $0.6 < x < 0.8$ tetragonal structure is thermodynamically unfavourable in hydrothermal reaction, or there is a miscibility gap in the $BaTiO_3$–$SrTiO_3$ system [4]. Fig. 11 shows the structural parameters of all the two-phase samples in this study. It clearly exhibits a gap $0.6 < x < 0.8$. This gap may be even wider to $0.6 < x < 0.9$ as $x = 0.81$ and 0.85 calculated from the peak fit (Table 1a and b) were not consistent with the whole spectrum fit. This might be caused by a presence of a minor third phase, which upsets the calculation.

Table 3
Data obtained from the XRD analysis of the (1 1 0) peaks of samples prepared with different time of the hydrothermal reaction

Time	2-th$_1$	2-th$_2$	S_1/S_2	t_1	t_2	x_1	x_2	Ba loss (%)
8	31.56	31.87	67/33	21	16	1.03	0.67	−1
12	31.60	31.96	86/14	20	17	1.01	0.55	−2
16	31.62	31.92	71/29	20	19	0.98	0.60	3
20	31.63	32.01	86/14	20	20	0.97	0.49	0
24	31.64	31.94	83/17	21	17	0.96	0.58	1
48	31.63	32.04	92/8	27	31	0.97	0.45	−3

Time of the reaction is given in hours, 2-th$_1$ and 2-th$_2$ are positions of the first and second peaks calculated from the peak fit, S_1/S_2 are relative areas under the peaks, t_1 and t_2 are sizes of the crystals calculated according to the formula (1) in nm, parameters x_1 and x_2 show amount of Ba in $Ba_xSr_{1-x}TiO_3$ compounds and are obtained from 2-th and Vegard's law (Fig. 2), Ba loss shows how much of Barium in the final product is unaccounted for compare with the initial value of 90% in percent.

In general, the obtained results agree with Ref. [4] on low temperature hydrothermal reaction. If there is a small deficiency in TiO_2, then BST is a two-phase solid solution. Calculations show that when the amount of Sr in the initial solution is above 30% the final compound has a structure of more than two phases.

4.5. Reaction time

It was found that the duration of reaction did not have a great influence on the composition of the final products. Six samples were prepared with a Ba:Sr initial mol ratio of 0.9:0.1 and (Ba + Sr)/TiO_2 = 0.25 for 8, 12, 16, 20, 24 and 48 h reaction time. The final parameters are listed in Table 3 and the XRD peaks are shown in Fig. 12. It can be seen that all the samples had two phases. The sample treated for 8 h did not fully react, as the XRD spectrum revealed traces of TiO_2, and the parameter x, calculated from the 2θ position of the first phase peak was 1.03, greater than unity. This means that the relation between Ba + Sr (A) and Ti (B) in the compound was not stoichiometric ABO_3. All final Ba:Sr ratios, calculated as above (4), were close to the initial 0.9:0.1. There was also little diffusion of Sr into the first phase with time as x_1 changed from 1.03 to 0.97. The crystal size of the phases remained small during the first 24 h,

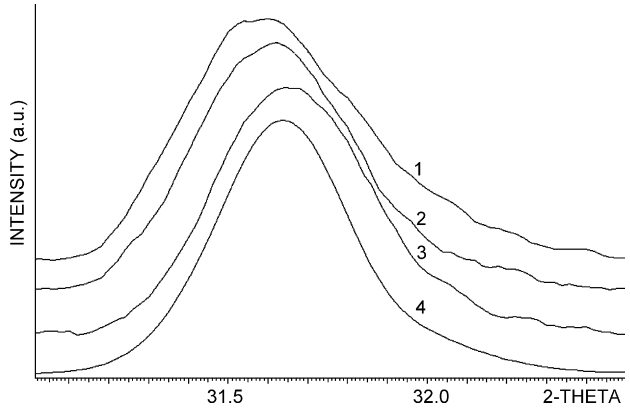

Fig. 12. (1 1 0) peak of samples prepared for 8, 12, 24 and 48 h (1–4), respectively. The peaks are smoothed and shifted vertically for a better view.

reflecting the phase nucleation, and then the growth rate increased sharply.

These results are different from the low temperature (80 °C) hydrothermal reaction results [4], in which the Sr-rich phase was first to appear, and the Ba-rich phase was only detected after 24 h, and continued to increase in volume up to 1200 h reaction.

5. Discussion

The experimental results were obtained under the following assumptions:

(a) the XRD peaks were considered as double peaks if their maximum did not coincide with their gravity centre,
(b) the relative area under the calculated peaks S_1/S_2 reflected the relative amount of the phases, and
(c) Vegard's law could be used for calculating x parameters of the phases.

In the (a) case the majority of the peaks were double headed and only a few peaks needed special attention. The case (b) means that we assumed a linear dependence between the area under the peak versus a relative share of the phase in the mixture. This is because a standard experimental calibration curve, when a known amount of the compounds is mixed, could not be acquired. The degree of an error though should not be high, as the phases have very similar crystal structures. The last assumption (c) is based on a high accuracy of lattice parameter measurements of the listed database data and almost linear dependence of $x(d)$ (Fig. 2). Roeder and Slamovich [4] argued that the experimental data obtained from the WDS measurements should be used instead of Vegard's law. In our experiments this data could not be applied, as our samples contained two phases. There is also a source of error in the peak fitting calculations. All together the absolute values of the obtained results may have a significant error and should not be used for a precise quantitative analysis but can be quite suitable for a qualitative understanding of hydrothermal reaction processes.

Fig. 11 shows that the tetragonal $Ba_xSr_{1-x}TiO_3$ compound with x in the range of 0.6–0.8 is a thermodynamically unfavourable structure, as the hydrothermal reaction prefers to go towards producing almost Sr-free $BaTiO_3$ and cubic $Ba_xSr_{1-x}TiO_3$ with $x < 0.6$ (Tables 1 and 3). When the fraction of Ba in the initial solution decreased to 70%, a third phase appeared. If the amount of Ti is insufficient for the formation of $BaTiO_3$ then a single phased $Ba_xSr_{1-x}TiO_3$, ''oversaturated'' above $x > 0.6$, may take place (Table 2 and Fig. 9). It is interesting to compare the results obtained from the Ba:Sr mol ratio and the (Ba + Sr):TiO_2 ratio experiments (Tables 1 and 2). Fig. 9 shows that even when the Ba:Sr mol ratio is high 0.9:0.1, Ba needs a high concentration of Ti to fully react. As the fraction of Sr increases (Fig. 8), it outperforms Ba due to its higher mobility and Ba losses increase linearly with Sr concentration. Fig. 8 shows that for every percent of introduced Sr there is a 1.6% loss of Ba. Sr is first to react with Ti, and as a result, decreases the TiO_2 concentration in the solution (Fig. 9), further increasing Ba losses.

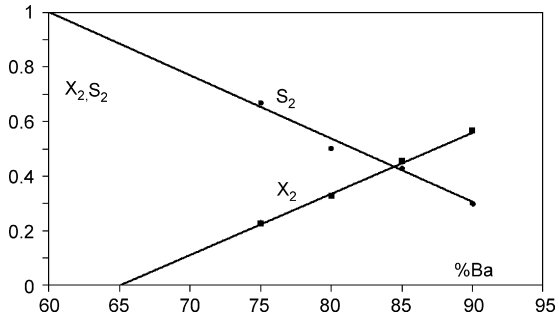

Fig. 13. Relative value of the area under the second peak S_2 (Table 1b) and its barium content x_2 vs. the amount of Ba (mol ratio) in the initial solution in percent. The extrapolations show that barium disappears from the second phase at 66%, and the whole sample structure becomes single-phased ($S_2 = 100\%$, $S_1 = 0$) at 61%.

We can also make some estimation from extrapolation of the obtained data (Table 1b) to low Ba values. It is seen from the extrapolation of S_2 and x_2 to S = 1 and $x = 0$ (Fig. 13), that the second phase becomes Ba-free ($x_2 = 0$) at 66%, and at a very close value of 61%, the whole structure becomes single phase.

6. Conclusions

Hydrothermal synthesis of barium strontium titanate at high temperature and elevated pressure showed similar results to that of a low temperature reaction [4]. Structure of the final BST product was greatly affected by two major parameters: Ba:Sr mol ratio and TiO_2 concentration. As Ba and Sr have different chemical activity and mobility, they react differently with Ti, leading to a multi-phase structure in the case of a small deficiency in Ti, and a single phase for a high deficiency in Ti. The threshold value of (Ba + Sr)/TiO_2 ratio for a single/two phase transition was about 3. The obtained phases were tetragonal $BaTiO_3$ and cubic $Ba_{0.6}Sr_{0.4}TiO_3$, if a relative share of Sr was small, less than 10%. As the amount of Sr increases it goes mostly to the cubic structure. When Sr concentration in the initial solution reaches 30%, the final BST becomes three phase. This process is also accompanied by Ba losses. For every introduced percent of Sr there is a 1.6% of Ba loss. The extrapolated data indicates that when the Ba:Sr ratio equals 0.61:0.39, there is almost no Ba left in the structure.

There was a difference between high and low temperature [4] hydrothermal reactions in BST formation with time. The analysis of the experimental data of high temperature reaction (Table 3) showed that the phase content of the final product stabilised quickly after the first 16–24 h. The crystal size remained very small, typical for the phase nucleation period, then was followed by crystal growth.

Acknowledgements

The authors would like to thank Dr. S. Panov for useful discussions. This research is partially supported by a NERF grant. One of the authors (KAR) appreciates the financial support from ASTS University Sains Malaysia.

References

[1] S. Tusseau-Nenez, J.-P. Ganne, M. Maglione, A. Morell, J.-C. Niepce, M. Pate, BST ceramics: effect of attrition milling on dielectric properties, J. Eur. Ceram. Soc. 24 (2004) 3003–3011.

[2] H.V. Alexandru, C. Berbecaru, A. Ioachim, M.I. Toacsen, M.G. Banciu, L. Nedelcu, D. Ghetu, Oxides ferroelectric (Ba, Sr)TiO_3 for microwave devices, Mater. Sci. Eng. B 109 (1–3) (2004) 152–159.

[3] A. Ries, A.Z. Simoes, M. Cilense, M.A. Zaghete, J.A. Varela, Barium strontium titanate powder obtained by polymeric precursor method, Mater. Charact. 50 (2003) 217–221.

[4] R.K. Roeder, E.B. Slamovich, Stoichiometry control and phase selection in hydrothermally derived $Ba_xSr_{1-x}TiO_3$, J. Am. Ceram. Soc. 82 (7) (1999) 1665–1675.

[5] S.B. Deshpande, Y.B. Khollam, S.V. Bhoraskar, S.K. Date, S.R. Sainkar, H.S. Potdar, Synthesis and characterization of microwave-hydrothermally derived $Ba_{1-x}Sr_xTiO_3$ powders, Mater. Lett. 59 (2–3) (2005) 293–296.

[6] J.I. Clark, T. Takeuchi, N. Ohtori, D.C. Sinclair, Hydrothermal synthesis and characterization of $BaTiO_3$ fine powders: precursors, polymorphism and properties, J. Mater. Chem. 9 (1999) 83–91.

[7] B.L. Newalkar, S. Komarneni, Microwave-hydrothermal synthesis and characterization of barium titanate powders, Mater. Res. Bull. 36 (2001) 2347–2355.

[8] P. Pinceloup, C. Courtois, A. Leriche, B. Thierry, Hydrothermal synthesis of nanometer-sized barium titanate powders: control of barium/titanium ratio, sintering, and dielectric properties, J. Am. Ceram. Soc. 82 (11) (1999) 3049–3056.

[9] S.-F. Liu, I.R. Abothu, S. Komarneni, Barium titanate ceramics prepared from conventional and microwave hydrothermal powders, Mater. Lett. 38 (5) (1999) 344–350.

[10] K.A. Razak, A. Asadov, J. Yoo, W. Gao, M. Hodgson, E. Haemmerle, Characterization of BST produced by high temperature hydrothermal synthesis, in: Proceedings of the Advanced Materials Development and Performance, 2005, p. 45.

[11] K.A. Razak, A. Asadov, J. Yoo, E. Haemmerle, W. Gao, Structural and electrical properties of barium strontium titanate (BST) produced by hydrothermal method, in: Proceedings of the First International Symposium on Functional Materials, 2005.

[12] D. Hennings, S. Schreinmacher, Characterization of hydrothermal barium titanate, J. Eur. Ceram. Soc. 9 (1992) 41–46.